PCCP
Physical Chemistry Chemical Physics

Accepted Manuscript

This article can be cited before page numbers have been issued, to do this please use: M. Abu-samha, P. Wang, T. X. Carroll, L. J. Sæthre and K. J. Borve, *Phys. Chem. Chem. Phys.*, 2026, DOI: 10.1039/D6CP00887A.

View Article Online
DOI: 10.1039/D6CP00887A

PCCP

ARTICLE TYPE

Cite this: DOI: 00.0000/xxxxxxxxxx

Oxygen 1s Photoelectron Spectroscopy of Gaseous Alcohols and the σ-Inductive Properties of Alkyl Groups†

Mahmoud Abu-samha,[a‡] Peng Wang,[b‡§] Thomas X. Carroll,[c] Leif J. Sæthre,[b] and Knut J. Børve*[d]

Received Date
Accepted Date

DOI: 00.0000/xxxxxxxxxx

This study presents a comprehensive investigation of alcohol molecules in the gas phase using oxygen 1s X-ray photoelectron spectroscopy (O1s XPS), complemented by carbon 1s XPS. We report ionization energies for a diverse set of aliphatic, alicyclic, aromatic, and unsaturated alcohols with an accuracy of 0.02 eV (O1s) and 0.035 eV (C1s). The resulting dataset provides a benchmark for electronic structure theory, a reference for spectroscopic analyses, and high-quality input for machine-learning models. By decomposing the ionization energies into initial- and final-state contributions, O1s chemical shifts are used to explore the electronic role of hydrocarbon substituents in alcohols. Among aliphatic and alicyclic alkyls, the capacity to donate electrons through σ-bond polarization in the neutral molecule was found to increase systematically through the sequence from methyl, via branched and linear primary alkyls, to secondary alkyls, and *tert*-butyl.

1 INTRODUCTION

Oxygen-containing functional groups play a central role in organic chemistry, and the hydroxy group serves as a particularly illustrative example. Alcohols — defined as compounds in which a hydroxy group is attached to a saturated carbon atom of an alkyl or cycloalkyl group (substituted or unsubstituted) (R-OH) — provide a valuable framework for studying the evolution of polarity and polarizability with the nature of R.

This study centers on isolated alcohol molecules and pursues two main objectives: (i) to report highly accurate O1s ionization energies for a structurally diverse set of alcohols, and (ii) to elucidate how polarity and polarizability vary with the hydrocarbon moiety bound to oxygen. O1s XPS offers an oxygen-site-specific probe with high sensitivity to the local electronic environment (see Fig. 1).

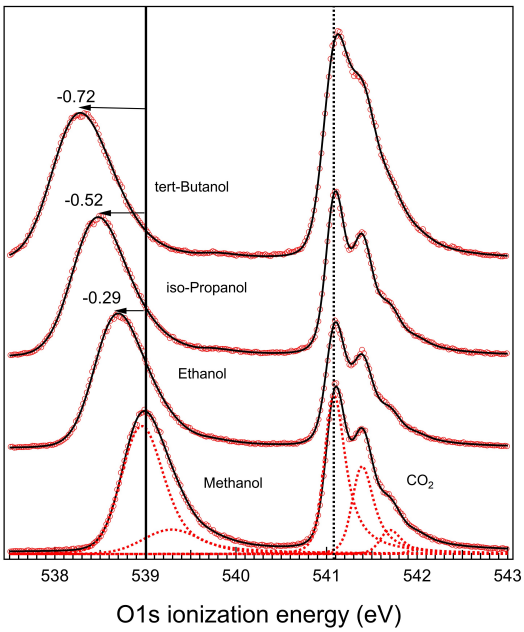

Fig. 1 Oxygen 1s photoelectron spectra of methanol, ethanol, *iso*-propanol and *tert*-butanol, each mixed with carbon dioxide. The circles are experimental data, and solid lines are the results from fitting. The CO_2 main (adiabatic) peak is used for internal calibration as indicated by the vertical dotted line. Chemical shifts in O1s ionization energy, relative to that of methanol, are indicated by horizontal arrows labeled by the shift values (in eV) for ethanol, *iso*-propanol and *tert*-butanol. The vibrational fitting model for CO_2 and the empirical two-peak model for methanol are indicated in dotted lines in the bottom spectrum.

* *Corresponding author.*
[a] *College of Integrative Studies, Abdullah Al Salem University, Khaldiya, Kuwait.*
[b] *Department of Chemistry, University of Bergen, NO-5007 Bergen, Norway.*
[c] *Division of Natural Sciences and Mathematics, Keuka College, Keuka Park, New York 14478, USA.*
[d] *Department of Chemistry, University of Bergen, NO-5007 Bergen, Norway. Tel: 47 5558 3365; E-mail: knut.borve@uib.no*
† *Electronic supplementary information (ESI) available: The ESI contains extended experimental details (Tab.1S (O1s), Tab. 2S (C1s)), O1s and C1s photoelectron spectra (Figs. S1 and S2) and a complete list of C1s energies (Tab. S3), and further details on the evaluation of Extended Koopmans' theorem energies. See DOI: 10.1039/cXCP00000x/*
‡ *These authors contributed equally to this work.*
§ *Present address: Room 909, Zhongdian Xinxi Building, Haidian District, Beijing, China.*

View Article Online
DOI: 10.1039/D6CP00887A

In the photoelectron experiment, the O1s ionization energy is measured by exposing the sample to highly monochromated photons of energy $h\nu$ and measuring the kinetic energy of the emitted electrons. While modern third- and fourth-generation synchrotron-radiation facilities offer very bright X-rays which in turn allow for a high degree of monochromatization, accuracy remains a problem. Advances in internal calibration[1] enable O1s ionization energies accurate to ± 0.02 eV across eight lower aliphatic alcohols (up to C4), four higher linear aliphatic alcohols (n-pentanol, 3-pentanol, n-hexanol, n-octanol), one alicyclic, one aromatic and two unsaturated alcohols (cyclohexanol, benzyl-, allyl- and propargyl alcohol), and phenol. The present dataset - unprecedented in combined accuracy and diversity - supports spectral assignment, development of machine learning models,[2] and benchmarking of electronic structure methods[3–5] that are now approaching and surpassing the accuracy of legacy compilations.[6]

The second main objective of the study, to explore how polarity and polarizability evolve in alcohols as a function of the hydrocarbon moiety hosting the hydroxy group, can be approached both experimentally and computationally. Computationally, polarity and polarization are often inferred from the molecular charge distribution, which can partitioned into atomic or group contributions using population analysis or topological methods[7]. However, such results are highly sensitive to the choice of basis set and the specific flavor of population analysis employed.[8] Experimentally, the interference of atomic charges typically relies on a model relating spectroscopic observables to the underlying charge distribution, and core-level ionization energies were early on interpreted within an electrostatic potential model. Later, Koopmans' theorem became an indispensable tool, stating that the energy required to ionize an electron from core orbital *O1s* is, apart from a sign reversal, approximately equal to the corresponding Hartree-Fock orbital energy ε_{1s} as computed for the neutral molecule. Unfortunately, the validity of this relationship is quite limited, as it requires both electron correlation and electronic relaxation in the ionized molecule to be negligible.

To obtain structure-property insight from core ionization energies (IE), we conceptually separate the ionization event into two consecutive steps: (i) removal of an O1s electron from an otherwise frozen electron configuration, followed by (ii) electronic relaxation of a molecule with an O1s vacancy. The *IE* may be decomposed accordingly, into an initial-state contribution V and a final-state contribution R, yielding $IE = V - R$.[9] The negative sign is chosen to reflect that any relaxation process in the final state will act to reduce the ionization energy. V is computed by means of an extension to Koopmans' theorem (the extended-Koopmans'-theorem; EKT)[10] which provides the energy cost of ionizing a core electron from the frozen, valence-electron-correlated neutral ground state. This approach provides a consistent and physically grounded framework for analyzing trends in polarity and polarizability across a diverse set of alcohols, which in turn reflect the electron-withdrawing or -donating ability of the hydrocarbon entity to which the hydroxy group is attached.

We will be concerned with the difference in ionization energy (ΔI) between differently substituted alcohols, such that $\Delta I = \Delta V - \Delta R$. The oxygen atom being probed is the point of attachment for the hydrocarbon substituent in the alcohol. By design, V reflects the charge distribution in the neutral molecule and is a key to the inductive properties of substituents. R, on the other hand, comprises orbital contraction at the ionized atom (O^*), through-bond electron transfer to O^*, and through-space polarization; cancellation of atomic terms renders ΔR a sensitive reporter of substituent polarizability.[9]

To illustrate the importance of final-state relaxation, it is instructive to review a recent example[11] where carbon 1s ionization energies were used to assess the properties of methyl as a substituent. In propyne, the C1s IE at C2 lies 0.32 eV below that of ethyne,[12] and it is tempting to take this as evidence for Me acting as an electron-releasing substituent, compared to H, when bonded to an ethynyl moiety. However, most of this negative shift arises from final-state relaxation ($\Delta R = 0.25$ eV), rather than from the charge distribution in the neutral molecule. In this particular case, the initial-state contribution to the shift remains negative, albeit small ($\Delta V = -0.07$ eV),[12] and thus supports Me acting as a weakly electron-releasing substituent.

The inductive character of alkyl substituents has been a subject of debate since the early days of physical organic chemistry, with alcohols providing a key source of experimental insight.[13–20] Early investigations established that alkyl groups primarily impart polarizability, rather than intrinsic polarity, to neutral molecules and to their gas-phase ionization behavior. To separate inductive contributions from dominant polarizability, Taft and co-workers employed isodesmic reactions, reporting appreciable electron-releasing effects of alkyl substituents relative to methyl.[15] Later studies, however, revised this interpretation. As substituent effects were systematically parameterized, alkylation — the substitution of hydrogen by an alkyl group — was found to impart negligible through-space dipolar field effects and minimal through-σ-bond charge transfer.[21,22] This perspective effectively stripped alkyl groups of significant inductive or polar character beyond their polarizability and capacity for hyperconjugation when attached to an extended π system.

Noteworthy, the term *inductive effect* has been used differently by different authors, some of whom includes through-space field effects and hyperconjugation.[23] However, for alkyls bonded to the hydroxy group in neutral alcohols, neither of these contributions is considered of importance.

Recently, it has been argued that alkyls are weakly and uniformly electron-withdrawing when compared to hydrogen, with the inductive effect defined as polarization of σ-bonds in neutral molecules.[11,20,24–26] Elliott *et al.* made an effort to uncover trends in the inductive effect of different alkyls in neutral organic molecules.[26] While concluding negatively based on computed atomic charges, they advised to consider the merit of other potential approaches to this issue. In this account, O1s XPS is used as a direct probe of the local electronic environment at oxygen in alcohols. By decomposing the measured O1s chemical shifts into initial-state (ΔV) and final-state (ΔR) contributions, we gain separate access to the local charge distribution at oxygen and to the polarizability of the hydrocarbon substituent. Comparing ΔV across a structurally diverse set of alcohols allows us to rank the

View Article Online
DOI: 10.1039/D6CP00887A

σ-inductive electron-donating or -withdrawing capacity of alkyl groups, while ΔR offers a complementary measure of substituent polarizability. The approach is further extended to selected unsaturated hydrocarbon substituents, where additional electronic contributions beyond pure σ-induction come into play.

2 METHODS

2.1 Experimental Procedures

O1s spectra of phenol and 16 alcohol molecules were recorded at beamline I411 of the MAXlab synchrotron facility.[27,28] The photon energy was approximately 580 eV. The analyzers were placed at 90° to the beam and 54.7° to the polarization direction. The kinetic energy scale was calibrated using the Xenon $N_{4,5}OO$ Auger spectrum.[29] The ionization energy scale was set by mixing each alcohol with carbon dioxide and using the high-accuracy O1s adiabatic energy of CO_2 (541.085 (17) eV) as internal reference.[1] For the overall instrumental resolution, which was approximated by a Gaussian profile, the full width at half maximum (fwhm) ranged from 0.14 to 0.22 eV, depending on the specific settings used; see Tab. S1.†

The absolute uncertainty in the reported O1s ionization energies is determined from a combination of the uncertainty of the CO_2 reference value, 0.017 eV,[1] and the uncertainty of the observed shift relative to CO_2. For the present measurements the uncertainty in individual chemical shifts is $\leq$ 0.010 eV, and the uncertainty in absolute ionization energies is estimated to 0.02 eV.

C1s photoelectron spectra were recorded for all compounds (except for n-octanol), with experimental details and photoelectron spectra provided in the ESI.† The spectra exhibit a sharp and vibrationally structured peak around 292 eV which is assigned to the carbinol carbon and of interest in the present work. A second and largely unstructured peak is found some 1.5–2 eV lower in energy (not in methanol), consisting of overlapping signals from the other carbon atoms in the molecule. The overall uncertainty in the carbinol C1s ionization energies is estimated at 0.035 eV, combining the uncertainty of the CO_2 reference (0.03 eV)[30] and that of the relative shift ($\leq$0.02 eV).

2.2 Fitting Models

Because O1s spectra are dominated by lifetime broadening (see below) and extensive vibrational excitation, each alcohol exhibits a single broad, and nearly featureless peak envelope. Two empirical components sufficed to represent the envelope; the vertical energy was taken as the area-weighted mean of these components, see the bottom spectrum in Fig. 1. In some cases, the spectra revealed small water contaminations (0.3% - 6%). This was modeled explicitly, with the position of H_2O fixed by its known shift to CO_2.[1] In order to determine the O1s ionization energy of the alcohol under study, line-shape profiles representing the contributions of alcohol, carbon dioxide, and water, were fit to the measured spectra. For CO_2 and H_2O, we adopted literature Franck-Condon profiles[31,32] and lifetime widths (CO_2: 0.166 eV; H_2O: 0.160 eV).[1,31] The lifetime width was fixed at 0.170 eV for all alcohols. The effects of post-collision interaction and lifetime broadening were included as advocated by van der Straten *et al.*[33] The parameters left to be determined in least-squares fits to the observed spectra by means of the SPANCF fitting package,[34,35] were the positions and intensities for the line-shape components of the alcohol, the position and intensity of the adiabatic peak for carbon dioxide, the intensity of the water contribution, and a constant background. C1s spectra were analyzed in a similar manner, cf ESI† for details.

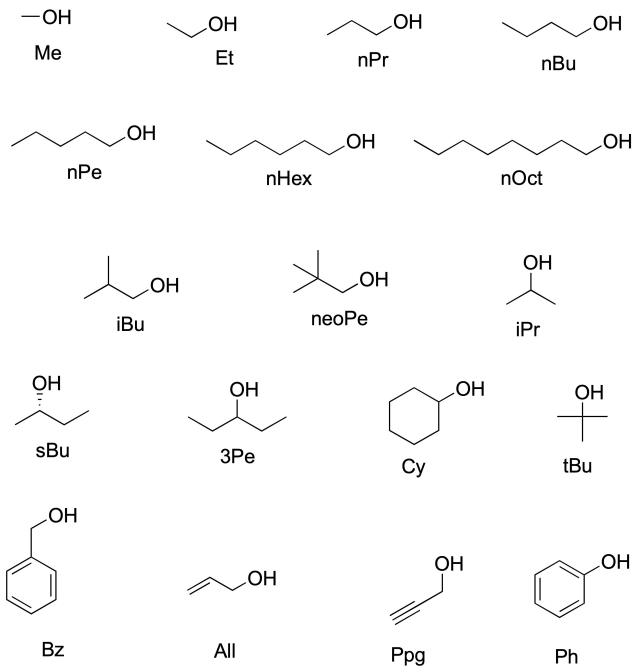

Fig. 2 Molecular structures of the compounds considered in this study, labeled using customary substituent abbreviations (nHex for n-hexyl, nOct for n-octyl, and otherwise as listed in Tab. 2).

2.3 Computational methods

Most of the alcohols studied here exhibit several low-energy conformers. To assess the influence of conformational equilibria on calculated initial-state shifts, a parallel study was carried out in which ΔV values were evaluated for individual conformers and for Boltzmann-weighted ensembles. For the purposes of the present work, conformational effects were found to be small and did not affect the qualitative trends or quantitative conclusions. We choose to report ensemble-averaged ΔV values; further details will be presented elsewhere,[36] including molecular structures as optimized using frozen-core second-order Möller-Plesset perturbation theory (MP2) with Dunning correlation-consistent basis sets of triple-ζ quality (cc-pVTZ)[37]. Fig. 2 presents the lowest-energy structures of the alcohols examined in this study.

Initial-state contributions to O1s and C1s ionization energies were computed in the extended-Koopmans'-theorem model by evaluating Eq. 2 in Ref. 10 using 1-particle reduced density matrices at the coupled clusters level of theory including single and double excitations (CCSD).[38] The calculations were performed with an in-house code[39] based on the PySCF framework,[40] using

View Article Online
DOI: 10.1039/D6CP00887A

aug-cc-pVTZ bases. Aside from a constant offset, the results agree well (cf ESI†) with those obtained with an approximate yet more pedagogical model (eq. 3 in Ref. 10): $V_{1s} = -\varepsilon_{1s} + eU_*^{MP2} - eU_*^{HF}$. Here, ε_{1s} is the O1s (C1s) orbital energy and U_* denotes the electrostatic potential at the site of ionization ((oxygen or carbon nucleus), computed using Hartree-Fock and frozen-core MP2, respectively. ΔV is formed by subtracting the corresponding value for methanol.

3 RESULTS

The results section is organized in three parts. Sec. 3.1 presents the measured O1s and C1s ionization energies and establishes the experimental chemical shifts that form the foundation of the analysis. In Sec. 3.2, these shifts are decomposed into initial (ΔV) and final-state (ΔR) contributions, separating the polarity induced by each substituent from its contribution to polarization in response to core ionization. Together, the two parts build the quantitative picture of substituent effects that is introduced in Sec 3.3 and explored in the Discussion section.

3.1 Oxygen 1s and Carbon 1s Ionization Energies

The study reports high-resolution O1s and C1s X-ray photoelectron spectra of a wide range of alcohols and phenol, encompassing linear, branched, secondary, tertiary, unsaturated, and aromatic compounds. Representative O1s spectra (methanol, ethanol, *iso*-propanol, and *tert*-butanol) are shown in Fig. 1 and serve to illustrate characteristic spectral features, the fitting methodology, and chemical shifts relative to methanol. All O1s spectra are available in the ESI.† Oxygen 1s ionization leads to significant elongation of the R–O bond, which in turn contributes to a broad and featureless spectral profile leaving the vertical ionization energy as the main observable. Accurate ionization energies were determined with an estimated uncertainty of 0.02 eV, using CO_2 as a calibration standard[1].

The measured O1s ionization energies are reported in Tab. 1. For five of the alcohols, namely *iso*-butanol, n- and 3-pentanol, n-hexanol, and propargyl alcohol, their oxygen 1s ionization energies have, to the best of our knowledge, not been reported before. For the other twelve compounds, our ionization energies (IE) generally agree well within error bars with earlier studies,[41–44] cf a detailed comparison in Appendix A. With the uncertainty associated with the CO_2 reference energy canceling when forming differences, chemical shifts relative to methanol are reported with high precision ($\leq$0.010 eV uncertainty) in Tab. 1. Although C1s is usually the preferred core for ionization when applying XPS to organic compounds, it is frequently complemented by heteroatom XPS.[45] For the purpose of exploring substituent effects in alcohols, the roles are switched as O1s XPS carries the significant advantage of probing the very site of attachment, oxygen. However, for a closer investigation of the polarity of the C–O bond, it is of interest to compare C_{OH}1s and O1s ionization energies. To this end, C1s photoelectron spectra have been recorded for all compounds in this study (except for n-octanol), with C1s spectra provided in the ESI.† The resulting carbinol C1s ionization energies, many of which are reported for the first time, are compiled in Tab. 1.

A simple observation from Tab. 1 is that within the set of saturated alcohols, O1s and C1s shifts span essentially the same interval, from 0.0 to -0.7 eV. This is mildly surprising, since the chemical changes upon substitution necessarily take place closer to the carbinol carbon than to the hydroxy oxygen. Fig. 3(a) compares shifts in C_{OH}1s and O1s ionization energies for the same aliphatic alcohols, relative to the corresponding signals in methanol. O1s shifts belonging to alcohols of different degree of substitution are resolved into non-overlapping intervals. From Tab. 1, primary alcohols (i.e. excluding methanol) display O1s energies from -0.29 to -0.48 eV relative to methanol, followed by secondary alcohols (-0.52 to -0.68 eV) and *tert*-butanol (at -0.72 eV). This is in contrast to the C1s data, where alcohols of different degrees may display nearly the same shift, as illustrated by n-propanol and *tert*-butanol sharing the carbinol C1s energy within 0.03 eV.

Within the same class of alcohols, the O1s and C1s shifts are closely correlated, with the C1s shifts being larger by a factor of two or more. From an analytical perspective, the O1s shifts provide a clearer separation between alcohols differing in the degree of substitution, whereas the C_{OH}1s shifts offer enhanced resolving power within a given class. To analyze these differences and to facilitate a discussion of substituent effects, we turn to a decomposition of chemical shifts into initial- and final-state contributions.

3.2 Initial- and final-state contributions to O1s and C1s ionization energies

It is conceptually desirable and computationally feasible to resolve chemical core-level shifts into initial- and final-state contributions according to $\Delta I = \Delta V - \Delta R$.[9] The initial-state contribution ΔV reflects the charge distribution in the neutral molecule and is largely determined by the change in electric potential upon substitution. Koopmans' theorem extended to included electron correlation effects[10] has been applied to compute the initial-state shifts compiled in Tab. 1 for both O1s and carbinol C1s. Combining experimental ΔI with computed ΔV produces semi-empirical values for the corresponding relaxation shift ΔR, also provided in the Table.

In Fig. 3(b), O1s and carbinol C1s shifts are resolved into (C1s,O1s) pairs of ΔV and ΔR data for each alcohol. Final-state relaxation is closely correlated between the two sites of ionization ($R^2 = 0.99$) and gives the dominant contribution to the chemical shift in both cases. As might be anticipated, ΔR is larger for C1s than O1s (by 45%), reflecting the difference in mean distance between the core hole and the polarizable substituent. For C1s, the larger relaxation is partly canceled by the positive ΔV, whereas for O1s, initial- and final-state contributions act in the same direction, thus explaining why C1s and O1s shifts span close to the same interval.

Fig. 3(b) also highlights that ΔV is of opposite sign for oxygen and the carbinol carbon; an alkyl substituent that lowers the potential at O also increases it at C_{OH}. However, the magnitude of the changes is five times larger at C_{OH}, compared to O, at odds with expectations within a simple bond-dipole model. This is-

View Article Online
DOI: 10.1039/D6CP00887A

Table 1 Measured vertical ionization energies (IE, eV), chemical shifts relative to methanol (ΔI, eV), calculated initial-state contributions (ΔV, eV), and final-state contributions ($\Delta R = \Delta V - \Delta I$, eV), for the O1s and C1s core levels respectively, pertaining to the C–O bond.

	Oxygen 1s				Carbinol C1s			
Alcohol	**O1s IE**	ΔI	ΔV	ΔR	**C1s IE**	ΔI	ΔV	ΔR
Primary Alcohols								
Methanol	538.988	0.000	0.000	0.000	292.458	0.000	0.000	0.000
Ethanol	538.698	-0.290	-0.065	0.225	292.298	-0.160	0.154	0.314
n-Propanol	538.619	-0.368	-0.066	0.302	292.127	-0.331	0.088	0.419
n-Butanol	538.575	-0.412	-0.072	0.340	292.030	-0.428	0.083	0.511
n-Pentanol	538.539	-0.449	-0.075	0.374	292.009	-0.448	0.082	0.530
n-Hexanol	538.529	-0.459	–	–	291.981	-0.477	–	–
n-Octanol	538.512	-0.475	–	–	–	–	–	–
iso-Butanol	538.560	-0.427	-0.052	0.375	291.941	-0.517	0.056	0.573
neo-Pentanol	–	–	-0.030	–	291.875	-0.583	0.050	0.633
Secondary Alcohols								
iso-Propanol	538.469	-0.519	-0.113	0.406	292.195	-0.263	0.321	0.584
sec-Butanol	538.387	-0.601	-0.115	0.486	292.020	-0.438	0.255	0.693
3-Pentanol	538.319	-0.669	-0.118	0.551	291.846	-0.612	0.191	0.803
Cyclohexanol	538.311	-0.677	-0.135	0.542	291.786	-0.672	0.160	0.832
Tertiary Alcohols								
tert-Butanol	538.264	-0.724	-0.156	0.568	292.156	-0.302	0.499	0.801
Unsaturated and Aromatic Alcohols								
Benzyl alcohol	538.556	-0.432	0.097	0.529	292.152	-0.306	0.374	0.680
Allyl alcohol	538.746	-0.242	0.091	0.333	292.393	-0.065	0.353	0.418
Propargyl	539.008	0.020	0.358	0.338	293.229	0.771	1.079	0.308
Phenols								
Phenol	539.203	0.215	0.913	0.698	292.024	-0.433	0.879	1.312

[a] Uncertainty: O1s IE $\approx$ 0.02 eV ; C1s IE $\approx$ 0.035 eV; O1s $\Delta I \leq$ 0.010 eV; C1s $\Delta I \leq$ 0.02 eV

View Article Online
DOI: 10.1039/D6CP00887A

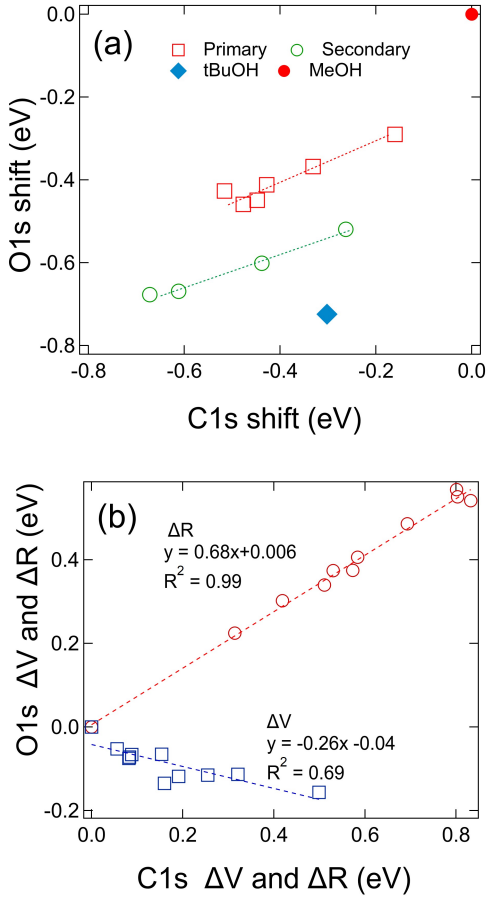

Fig. 3 Comparison of C1s and O1s shifts for the atoms in the C–O bond in aliphatic alcohols, relative to those of methanol. All energies in eV. (a) Each data point represents an alcohol according to (ΔI_{C1s}, ΔI_{O1s}). (b) ΔI is decomposed into initial- (ΔV, squares) and final-state (ΔR; circles) contributions, with C1s (O1s) data referring to the abscissa (ordinate axis).

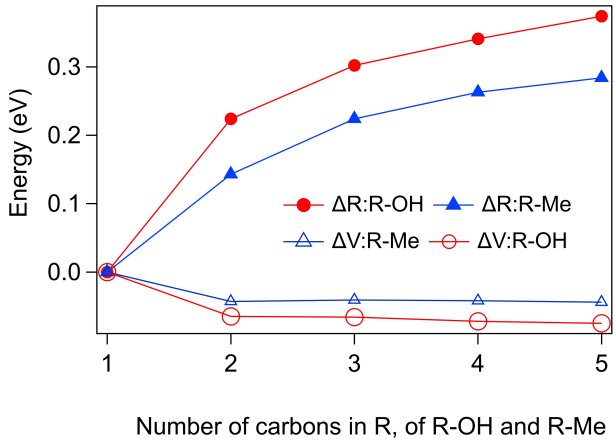

Fig. 4 Initial-state (ΔV, open symbols) and final-state contributions (ΔR, filled symbols) to the chemical shift in core ionization energy of oxygen in n-alkanols R-OH (O1s IE relative to methanol) and the methyl carbon in linear alkanes R-Me (C1s IE relative to ethane). The data pertain to all-*trans* conformers. ΔV for C1s is computed in this work, with ΔR obtained by subtracting the experimental shifts reported in Ref. 46.

sue is resolved by noting that C1s energies report from *within* the substituent, and modifying the alkyl substituent affects the C_{OH}1s energy more profoundly than what is reflected at the oxygen site, effectively making C1s shifts and the associated initial-state shift ΔV less suitable for characterizing the hydrocarbon substituent in the alcohol. To clarify, C1s is a preferred core level when using functionalized methanes[47] or benzenes[48] as scaffolds for comparing hetero substituents. Along the same line of reasoning, one may consider methyl groups in an alkane for potential probes of the complementary alkyl, to be explored next.

Fig. 4 shows the relative importance of initial- and final-state contributions to O1s shifts in n-alkanols (R-OH) and how they evolve with the length of the alkyl group R. Also included are C1s data for ionization of the terminal Me group of the corresponding alkane R-Me, obtained by replacing OH by Me. Pairs of O1s and C1s energies provide insight into what is formally the same alkyl substituent, apart from any differences imparted by OH and Me, respectively. The data are plotted against the number of carbons in the designated R substituent. From Fig. 4, final-state relaxation is clearly the dominant contribution to chemical shifts in C1s IE in alkanes as well as in O1s IE in n-alkanols, both in terms of absolute numbers and evolution with molecular size. The larger ΔR value for the higher alcohols compared to n-alkanes may at least in parts be ascribed to the choice of methanol as a reference. Methanol is unique among the alcohols in retaining significant covalency in the C–O* bond, cf. Appendix A and Ref. 49, with correspondingly less final-state relaxation.

The close similarity of ΔV for the same alkyl group across the two homologous series, adds confidence in ΔV as a useful probe of substituent effects. Moreover, one is led to conclude that apart from any differences that may exist between Me in methanol (O1s) and in ethane (C1s), any further changes with the size of the linear alkyl substituent seem to take place to equal extent in alkanes and n-alkanols. The evolution with size is largely converged already with R=Et, as judged by the constancy of ΔV.

3.3 A substituent-oriented analysis of O1s shifts in aliphatic and alicyclic alcohols

In this section, the O1s-related energies in Tab. 1 are analyzed within a conceptual framework of substituent effects as manifested in the neutral molecule (initial-state effects) or as response to the charging event (final-state effects). For compactness and in preparation for a discussion of substituent effects, alcohols will henceforth be referred to by the corresponding hydrocarbon substituent, and more specifically by their customary abbreviations listed in Tab. 2, with OH added as a suffix.

3.3.1 Core ionization at the point of substitution - ΔR vs Taft's polarization parameter.

Taft and coworkers introduced the semi-empirical σ_α parameter to quantify the ability of a substituent to polarize in the field of a charge near the point of attachment.[18,22] In Fig. 5, our computed O1s ΔR values are plotted against $-\sigma_\alpha$ for the substituents and compounds of this study. Apparently, there is a strong and essentially linear relationship between the two quantities, to the extent that one of them may be used as a proxy for the other.

View Article Online
DOI: 10.1039/D6CP00887A

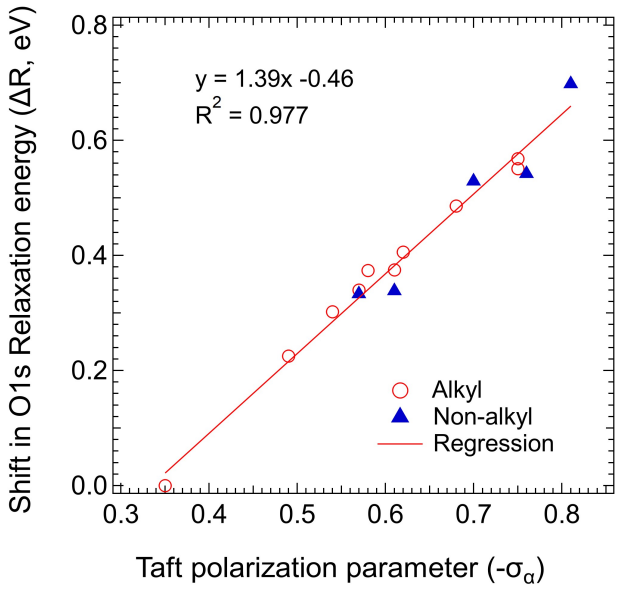

Fig. 5 Relaxation contribution, ΔR, to O1s IE relative to methanol, of alcohols (and phenol), plotted against Taft's polarization parameter ($-\sigma_\alpha$) for the corresponding substituents. Aliphatic alkyl substituents: Open circles; non-aliphatic substituents (Cy, All, Ppg, Bz, and Ph): Filled triangles. The embedded least-squares line is fit to all data. When applied to the aliphatic subset alone, $R^2 = 0.988$.

This result lends support to ΔR as a quantitative measure of polarizability and at the same time topicalizes σ_α as a practical tool in the analysis of core-level shifts. The latter point may be exemplified by reference to Fig. 5, where two pairs of alkyls stand out with nearly identical σ_α values and thus closely similar relaxation energies. Specifically, *tert*-butanol and 3-pentanol share $-\sigma_\alpha = 0.75$ [18,22], with the tertiary alcohol displaying the lower O1s IE by 0.055 eV. Similarly, *iso*-propanol and *iso*-butanol (2-methyl-1-propanol) have $-\sigma_\alpha$ values within 0.01 (0.62 and 0.61, respectively), where the O1s IE of the secondary alcohol lies 0.091 eV below that of the primary *iso*-butanol. Within each of these pairs, the chemical shift in O1s IE may thus be ascribed to initial-state effects alone, with the lower O1s IE of the more substituted alcohol indicating a more electron-rich oxygen. Taken together, these observations indicate that the electron-donating ability increases with the degree of substitution, following the trend $3^\circ > 2^\circ > 1^\circ$. This aspect will be investigated more systematically in the following.

3.3.2 Trends in O1s ΔV - initial-state polarity.

Inspection of Tab. 1 reveals that all aliphatic and alicyclic alcohols have a lower initial-state contribution to their O1s IE than do methanol. Moreover, the magnitude of ΔV increases quite smoothly from branched to linear primary alcohols, to secondary aliphatic alcohols and then to the only tertiary alcohol in the study, spanning a narrow interval of 0.16 eV. Still, there are noticeable steps corresponding to the degree of substitution. Thus, ΔV is essentially constant among the linear primary alcohols (ΔV=-0.070(5) eV), as well as for the aliphatic secondary alcohols (ΔV=-0.115(3) eV). Tertiary butanol has the most negative ΔV of the study, at -0.156 eV, and also the most negative shift in O1s ionization energy, at -0.724 eV.

For ease of reference, our computed O1s ΔV values are compiled in Tab. 2 along with the hydrocarbon substituent of the corresponding alcohol (or phenol). Focusing on aliphatic alkyl and cycloalkyl substituents, based on the initial-state shift relative to methanol, they cluster according to Me > neoPe > iBu > {Et, nPr, nBu, nPe} > {iPr, sBu, 3Pe} > Cy > tBu.

Table 2 Relative initial-state shifts (eV) in O1s ionization energies of *R-OH*

Substituent	ΔV^a (eV)
Methyl (Me)[b]	0.000
neo-Pentyl (neoPe)	-0.030
iso-Butyl (iBu)	-0.052
Ethyl (Et)	-0.065
n-Propyl (nPr)	-0.066
n-Butyl (nBu)	-0.072
n-Pentyl (nPe)	-0.075
iso-Propyl (iPr)	-0.113
sec-Butyl (sBu)	-0.115
3-Pentyl (3Pe)	-0.118
Cyclohexyl (Cy)	-0.135
tert-Butyl (tBu)	-0.156
Benzyl (Bz)	0.097
Allyl (All)	0.091
Propargyl (Ppg)	0.358
Phenyl (Ph)	0.913

[a] ΔV relative to methyl alcohol
[b] Abbreviation given within parentheses

3.3.3 Trends in O1s ΔR - final-state polarization.

The significant variations observed in the O1s chemical shifts are not primarily driven by the initial-state term, but instead arise from differences in final-state relaxation; ΔR. The systematic increase in ΔR with increasing size of the substituent — e.g., from 0.225 eV (Et) to 0.374 eV (nPe) for primary alcohols and from 0.406 eV (iPr) to 0.551 eV (3Pe) for secondary alcohols, points to enhanced polarization screening of the core hole, as is also confirmed by the close correlation between ΔR and Taft's polarization parameter of the corresponding hydrocarbon substituent, cf Fig. 5. The additive nature of ΔR is well illustrated in its evolution with increasing methylation at the carbinol carbon, from MeOH, via EtOH, iPrOH, and to tBuOH, in steps of 0.225, 0.181 and 0.162 eV, respectively, and averaging at 0.189 eV per methyl group. The secondary alcohols iPrOH, sBuOH and 3PeOH serve to illustrate the effect of distance from the site of ionization, as they may be related through methylation at one C–C bond removed from C_{OH}. According to Tab. 1, ΔR increases in steps of 0.080 and 0.065 eV, respectively. Similarly in a primary alcohol, methylating at one C–C bond removed from C_{OH} (EtOH → nPrOH) increases ΔR by 0.077 eV. The fall-off with distance of the ΔR contribution from a methyl group, is thus quite rapid, corresponding to a damping factor of 1-0.074/0.189 = 0.61 (61%). For comparison, in a computational study[50] of the propagation of substituent effects over an alkyl spacer, the authors found that there was no significant difference between Me and H beyond one C–C bond.

View Article Online
DOI: 10.1039/D6CP00887A

Taken together, the results of Sec. 3 establish a consistent and internally coherent picture of substituent effects in alcohols as probed by O1s XPS. The measured chemical shifts (ΔI) are dominated in magnitude by final-state relaxation (ΔR), which scales systematically with substituent size and correlates strongly with Taft's polarizability parameter σ_α. The initial-state contribution (ΔV), though smaller in magnitude, carries a chemically interpretable signal: it varies systematically with the degree of substitution and branching of the alkyl group, and is essentially insensitive to chain elongation beyond ethyl. This clean separation between polarizability (ΔR) and inductive capacity (ΔV) motivates the substituent-level interpretation developed in the Discussion.

4 DISCUSSION

The Discussion draws on the ΔV and ΔR values compiled in Tab. 1 to address two distinct aspects of substituent behavior. Section 4.1 focuses on the σ-inductive properties of aliphatic and alicyclic alkyls, interpreting the initial-state shifts (ΔV) in terms of through-bond charge polarization in the neutral molecule. Section 4.2 then turns to the unsaturated substituents — allyl, propargyl, benzyl, and phenyl — where hyperconjugation and resonance interact with σ-induction to produce qualitatively different behavior in both the initial- and final-state contributions. Throughout, O1s XPS is shown to provide a physically transparent and experimentally precise probe that distinguishes between these mechanistically distinct contributions to substituent effects.

4.1 The σ-inductive nature of alkyls

For the present set of compounds, oxygen 1s is the probe of choice for the local impact of the hydrocarbon substituent; the general idea being that the lower the atomic charge on oxygen, the less energy is required to core-ionize the atom. Furthermore, with a restrictive definition of the inductive effect as polarization of σ-bonds in the neutral molecule, it is the initial-state contribution to the O1s shift that is of relevance.

The electronic structure of simple aliphatic and alicyclic alcohols is dominated by localized σ-bonding and inductive effects associated with the electronegative oxygen atom, whereas resonance stabilization becomes important only in conjugated systems, to be discussed in the subsequent section. Since neither resonance effects nor hyperconjugation are expected to play a significant role in saturated alcohols, this allows for an interpretation in terms of σ-inductive substituent effects of the relative initial-state shifts provided in Tab. 2. With ΔV getting increasingly negative according to Me > neoPe > iBu > {Et, nPr, nBu, nPe} > {iPr, sBu, 3Pe} > Cy > tBu, the electron-donating capacities increase in the same order (with the inequalities reversed).

With Me as the least electron-donating (most electron-withdrawing) of the saturated alkyls, the branched primary alkyls (neoPe and iBu) have electron-donating capacities only marginally greater, and approaching that of Et and the higher linear alkyls, which all behave similarly. From the perspective of O1s ΔV, the secondary alkyls are indistinguishable in their electron-donating capacity, which is higher than any of the primary alkyls. The single tertiary alkyl in the data set is more electron-donating still. The increments between primary and secondary alkyls, and between secondary and tertiary ones, are quite similar. The alicyclic secondary substituent Cy comes out in-between tBu and the secondary alkyls, indicating that the structural constraint of the cycle enhances its electron-donating capacity as compared to the aliphatic secondary alkyls.

An interesting question concerns the electron-releasing capacity of hydrogen compared to the substituents listed in Tab. 2. Within an ROH framework, R=H corresponds to water rather than an alcohol. This aside, applying the extended Koopmans' theorem obtains a positive initial-state contribution to the O1s shift in water relative to methanol, of 0.092 eV. The immediate implication would be that H is electron-withdrawing compared to Me. However, even if the net charge on Me were equal to that of H in water, the difference between OH and OC bond lengths would make the electrostatic potential at the oxygen site significantly higher in water compared to methanol. Our computed ΔV for water includes this geometric effect as well as any changes in the atomic charges, most notably that of oxygen. Lacking a clear path to disentangle these contributions, our data alone do not allow insertion of H into the ΔV scale of Tab. 2 and still retain interpretability in terms of inductive capacity. The scientific case for alkyls being slightly electron-withdrawing, relative to H, when attached to an sp^3-hybridized site, is well argued in Refs. 11,25.

4.2 The electronic nature of unsaturated hydrocarbon substituents

4.2.1 Initial-state shifts.

The unsaturated substituents explored in this work, i.e., benzyl, allyl, propargyl and phenyl, all give rise to significantly higher initial-state contributions to the O1s shift than do any of the saturated alkyls. The bond-order isomers n-propanol, allyl alcohol and propargyl alcohol present a clarifying example, and from Tab. 2, nPr, All and Ppg instill initial-state contributions to the O1s shift relative to methanol (ΔV), of -0.07, +0.09 and +0.36 eV, respectively. Different from the neutral n-propanol, where hyperconjugation is unimportant, in the neutral allyl and propargyl alcohols, induction through the σ-bonds works in concert with hyperconjugation to transfer electron density from the hydroxylated carbon to the opposite end of the molecule, see the following dipolar resonance structures:

$$H_2C = CH - CH_2 - OH \;\leftrightarrow\; H_2C^- - CH = CH_2^+ - OH$$

and

$$HC \equiv C - CH_2 - OH \;\leftrightarrow\; HC^- = C = CH_2^+ - OH$$

Thus, hyperconjugation contributes significantly to positive initial-state contributions to O1s ionization in the two unsaturated alcohols, and much more so in PpgOH than in AllOH, on account of the much higher electron affinity of ethynyl over the vinyl group. Noteworthy, while ΔV may still be used to gauge the relative electron-releasing or -withdrawing capacity of All and Ppg, we are not in position to isolate the importance of (σ-)induction in these substituents.

Benzyl alcohol is both a primary and an unsaturated alcohol, al-

View Article Online
DOI: 10.1039/D6CP00887A

lowing for a hyperconjugative structure similar to the one drawn for allyl alcohol, whereby a negative charge is propagated to ortho positions: $Ph-CH_2-OH \leftrightarrow Ph^- = CH_2^+ - OH$. In phenol, the OH bond is polarized by hyperconjugation and resonance interactions, placing negative charge at the para carbon and positive charge near oxygen.

4.2.2 Final-state relaxation.

Hyperconjugation is expected to contribute significantly to final-state relaxation in substituents with H at the α carbon, as is additional resonance interaction in the unsaturated compounds. This may be illustrated by the series of nPrOH and its bond-order isomers AllOH and PpgOH, for which ΔR is constant or even slightly increasing, despite a falling number of valence electrons. For convenience, we will make use of the equivalent-cores approximation, whereby the core-ionized oxygen atom is formally represented by a valence-ionized fluorine atom, and the molecular ion by the resonance structures $R-F^+H \leftrightarrow R^+\cdots HF$.

In nPr^+, the net charge may be delocalized through hyperconjugation: $CH_3CH_2-CH_2^+ \leftrightarrow CH_3CH_2^+ = CH_2$. In All^+ and Ppg^+, bond-conserving resonance structures offer a significantly more efficient mechanism of charge delocalization; $H_2C=CH-CH_2^+ \leftrightarrow H_2C^+-CH=CH_2$ and $HC\equiv C-CH_2^+ \leftrightarrow HC^+=C=CH_2$. Thus, whereas unsaturated substituents have less electrons than their saturated counterparts, this may be more than compensated for by their efficient means of charge delocalization through bond-conserving resonance structures. In Fig. 5, a linear best-fit model in Taft's polarization parameter σ_α is seen to perform almost as well for the combined set of saturated and unsaturated substituents/compounds, as it is for the aliphatic alkyls alone, implying that σ_α successfully accounts for resonance contributions to polarization.

Conclusions

High-accuracy O1s ($\pm$0.02 eV) and C1s ($\pm$0.035 eV) ionization energies are reported for phenol and a structurally diverse set of alcohols, providing a benchmark dataset for electronic structure theory and machine-learning models. Decomposing O1s chemical shifts into initial- and final-state contributions ($\Delta I = \Delta V$ - ΔR) reveals two distinct and complementary aspects of substituent behavior: the initial-state component ΔV encodes the σ-inductive capacity of the hydrocarbon substituent in the neutral molecule, while ΔR quantifies its polarizability response to core ionization. The ΔV data provide evidence that the electron-donating capacity among alkyl substituents, increases systematically in the order Me < {1° branched} < {1° linear} < {2° aliphatic} < {2° Cy} < {3° tBu}. This reflects a clear and consistent dependence on degree of substitution and chain branching. Further work is required to explore the limit of validity of this systematic development in the σ-inductive effect of alkyls as substituents. The final-state component ΔR is found to correlate strongly and linearly with Taft's polarizability parameter σ_α across both saturated and unsaturated alcohols and phenol, validating σ_α as a physically grounded quantity and enabling a semi-empirical extension of the present ΔV-based framework to systems beyond those studied here.

Author contributions

Conceptualization (KJB), Data curation (LJS), Formal analysis (MA, PW, KJB), Funding acquisition (KJB), Investigation (all), Methodology (MA, KJB), Project administration (KJB), Resources (MA, KJB, LJS), Supervision (MA, TXC, LJS, KJB), Validation (all), Visualization (MA, PW, KJB), Writing – original draft (KJB) - review & editing (all).

Conflicts of interest

There are no conflicts to declare.

Data availability

The following data for this article are available as Electronic Supplementary Information: Extended experimental details of the recording of carbon 1s and oxygen 1s photoelectron spectra of gaseous alcohols and phenol, graphical representation of the same spectra, and details on the computational approach to computing initial-state shifts in core 1s ionization energies. The pyEKT computer program is available from the corresponding author upon request. See DOI: [URL – format https://doi.org/DOI]

Acknowledgements

The authors would like to acknowledge Mikko Erik Vedeler Saraste, Ingvild Isaksen and Karolina Solheimslid Eikås for their contributions to data acquisition as part of their thesis work. PW and KJB are grateful for support from the Norwegian Research Council by Grant No. 205512/F20, Nano-solvation in Hydrogen-Bonded Clusters. All quantum chemical calculations were performed on resources provided by Sigma2 - the National Infrastructure for High-Performance Computing and Data Storage in Norway - through project number NN2506K.

References

1 P. Wang, T. X. Carroll, T. D. Thomas, L. J. Sæthre and K. J. Børve, *J. Electron Spectrosc. Relat. Phenom.*, 2021, **251**, 147103–1–7.
2 F. Porcelli, F. Filippone, E. Colasante and G. Mattioli, *J. Chem. Phys.*, 2025, **162**, 244101.
3 J. Liu, D. Matthews, S. Coriani and L. Cheng, *J. Chem. Theory Comput.*, 2019, **15**, 1642–1651.
4 D. Golze, L. Keller and P. Rinke, *J. Phys. Chem. Lett.*, 2020, **11**, 1840–1847.
5 M. Huang and F. A. Evangelista, *J. Chem. Theory Comput.*, 2024, **20**, 7990–8000.
6 W. L. Jolly, K. D. Bomben and C. J. Eyermann, *At. Nucl. Data Tabl.*, 1984, **31**, 433–493.
7 J. Zhao, Z.-W. Zhu, D.-X. Zhao and Z.-Z. Yang, *Phys. Chem. Chem. Phys.*, 2023, **25**, 9020–9030.
8 S. C. North, K. R. Jorgensen, J. Pricetolstoy and A. K. Wilson, *Front. Chem.*, 2023, **11**, 1–20.
9 T. D. Thomas, *J. Electron Spectrosc. Relat. Phenom.*, 1980, **20**, 117–125.
10 K. J. Børve and T. D. Thomas, *J. Electron Spectrosc. Relat. Phenom.*, 2000, **107**, 155 – 161.
11 L. Salvatella, *J. Chem. Educ.*, 2025, **102**, 4666–4675.

View Article Online
DOI: 10.1039/D6CP00887A

12 L. J. Sæthre, N. Berrah, J. D. Bozek, K. J. Børve, T. X. Carroll, E. Kukk, G. L. Gard, R. Winter and T. D. Thomas, *J. Am. Chem. Soc.*, 2001, **123**, 10729–10737.
13 C. K. Ingold, *Structure and mechanism in organic chemistry.*, Cornell University Press, Ithaca, NY, 1953.
14 R. W. Taft, *J. Am. Chem. Soc.*, 1953, **75**, 4231–4238.
15 R. W. Taft, M. Taagepera, J. L. M. Abbound, J. F. Wolf, D. J. DeFrees, W. J. Hehre, J. E. Bartmess and R. T. McIver, Jr., *J. Am. Chem. Soc.*, 1978, **100**, 7765–7767.
16 J. E. Bartmess, J. A. Scott and R. T. McIver, Jr., *J. Am. Chem. Soc.*, 1979, **101**, 6056–6063.
17 G. Boand, R. Houriet and T. Gaumann, *J. Am. Chem. Soc.*, 1983, **105**, 2203–2206.
18 C. Hansch, A. Leo and R. W. Taft, *Chem. Rev.*, 1991, **91**, 165–195.
19 F. D. Proft, W. Langenaeker and P. Geerlings, *Tetrahedron*, 1995, **51**, 4021–4032.
20 O. Exner and S. Böhm, *Eur. J. Org. Chem.*, 2007, **17**, 2870–2876.
21 R. W. Taft and R. D. Topsom, *Prog. Phys. Org. Chem.*, 1987, **16**, 1–83.
22 R. W. Taft, I. A. Koppel, R. D. Topsom and F. Anvia, *J. Am. Chem. Soc.*, 1990, **112**, 2047–2052.
23 *IUPAC Compendium of Chemical Terminology*, ed. A. D. McNaught and A. Wilkinson, Blackwell Science, 2nd edn, 1997.
24 L. Salvatella, *Educación Química*, 2017, **28**, 232–237.
25 M. C. Elliott, C. E. Hughes, P. J. Knowles and B. D. Ward, *RSC Adv.*, 2025, **15**, 21780.
26 M. C. Elliott, C. E. Hughes, P. J. Knowles and B. D. Ward, *Org. Biomol. Chem.*, 2025, **23**, 352–359.
27 M. Bässler, J.-O. Forsell, O. Björneholm, R. Feifel, M. Jurvansuu, S. Aksela, S. Sundin, S. L. Sorensen, R. Nyholm, A. Ausmees and S. Svensson, *J. Electron Spectrosc. Relat. Phenom.*, 1999, **101-103**, 953–957.
28 M. Bässler, A. Ausmees, M. Jurvansuu, R. Feifel, J.-O. Forsell, P. de Tarso Fonseca, A. Kivimäki, S. Sundin, S. L. Sorensen, R. Nyholm, O. Björneholm, S. Aksela and S. Svensson, *Nucl. Instr. Meth. Phys. Res. A*, 2001, **469**, 382–393.
29 T. X. Carroll, J. D. Bozek, E. Kukk, V. Myrseth, L. J. Sæthre, T. D. Thomas and K. Wiesner, *J. Electron Spectrosc. Relat. Phenom.*, 2002, **125**, 127–132.
30 V. Myrseth, J. D. Bozek, E. Kukk, L. J. Sæthre and T. D. Thomas, *J. Electron Spectrosc. Relat. Phenom.*, 2002, **122**, 57–63.
31 R. Sankari, M. Ehara, H. Nakatsuji, Y. Senba, K. Hosokawa, H. Yoshida, A. D. Fanis, Y. Tamenori, S. Aksela and K. Ueda, *Chem. Phys. Lett.*, 2003, **380**, 647–653.
32 T. Hatamoto, M. Matsumoto, X.-J. Liu, K. Ueda, M. Hoshino, K. Nakagawa, T. Tanaka, H. Tanaka, M. Ehara, R. Tamaki and H. Nakatsuji, *J. Electron Spectrosc. Relat. Phenom.*, 2007, **155**, 54–57.
33 P. van der Straten, R. Morgenstern and A. Niehaus, *Z. Phys. D*, 1988, **8**, 35–45.
34 E. Kukk, G. Snell, J. Bozek, W.-T. Cheng and N. Berrah, *Phys. Rev. A*, 2001, **63**, 062702–1–9.
35 E. Kukk, K. Ueda, U. Hergenhahn, J. L. X, G. Prümper, H. Yoshida, Y. Tamenori, C. Makochekanwa, T. Tanaka, M. Kitajima and H. Tanaka, *Phys. Rev. Lett.*, 2005, **95**, 133001–1–4.
36 M. Abu-samha, P. Wang, L. J. Sæthre and K. J. Børve, In preparation.
37 R. A. Kendall, T. H. Dunning and R. J. Harrison, *J. Chem. Phys.*, 1992, **96**, 6796–6806.
38 G. E. Scuseria, C. L. Janssen and I. Schaefer, Henry F., *J. Chem. Phys.*, 1988, **89**, 7382–7387.
39 K. J. Børve, *pyEKT - A pyscf-based script for evaluating electronically vertical ionization energies in the extended-Koopmans approximation.*, 2026, University of Bergen, Norway.
40 Q. Sun, T. C. Berkelbach, N. S. Blunt, G. H. Booth, S. Guo, Z. Li, J. Liu, J. McClain, S. W. S. Sharma and G. K.-L. Chan, *WIREs Comput. Mol. Sci.*, 2018, **8**, e1340–1–15.
41 M. R. F. Siggel and T. D. Thomas, *J. Electron Spectrosc. Relat. Phenom.*, 1989, **48**, 101–116.
42 D. Nordfors, A. Nilsson, N. Mårtensson, S. Svensson, U. Gelius and H. Ågren, *J. Electron Spectrosc. Relat. Phenom.*, 1991, **56**, 117–164.
43 B. E. Mills, R. L. Martin and D. A. Shirley, *J. Am. Chem. Soc.*, 1976, **98**, 2380–2385.
44 F. M. Benoit and A. G. Harrison, *J. Am. Chem. Soc.*, 1977, **99**, 3980–3984.
45 A. J. R. Hensley, N. Cardwell, C. Jirausch, C. Papp, R. Denecke and J.-S. McEwen, *J. Phys. Chem. C*, 2025, **129**, 21938–21954.
46 T. Karlsen, K. J. Børve, L. J. Sæthre, K. Wiesner, M. Bässler and S. Svensson, *J. Am. Chem. Soc.*, 2002, **124**, 7866–7873.
47 O. Travnikova, S. Svensson, D. Céolin, Z. Bao and M. N. Piancastelli, *Phys. Chem. Chem. Phys.*, 2009, **11**, 826–833.
48 A. Hill, H. Sa'adeh, D. Cameron, F. Wang, A. B. Trofimov, E. Y. Larionova, R. Richter and K. C. Prince, *J. Phys. Chem. A*, 2021, **125**, 9877 – 9891.
49 J. K. Laerdahl, P. U. Civcir, L. Bache-Andreassen and E. Uggerud, *Org. Biomol. Chem.*, 2006, **4**, 135–141.
50 V. V. Divya, F. B. Sayyed and C. H. Suresh, *ChemPhysChem*, 2019, **20**, 1752–1758.
51 G. Johansson, J. Hedman, A. Berndtsson, M. Klasson and R. Nilsson, *J. Electron Spectrosc. Relat. Phenom.*, 1973, **2**, 295–317.
52 T. X. Carroll, M. R. F. Siggel and T. D. Thomas, *J. Electron Spectrosc. Relat. Phenom.*, 1988, **46**, 249–253.
53 T. X. Carroll, S. R. Smith and T. D. Thomas, *J. Am. Chem. Soc.*, 1975, **97**, 659–660.

A Experimental Oxygen 1s ionization energies

Oxygen 1s X-ray photoelectron spectra have been recorded with instrumental broadening (fwhm) of 0.22 eV or better, for seven linear n-alcohols (methanol– n-hexanol, & n-octanol), a branched primary alcohol (*iso*-butanol), three aliphatic and an alicyclic secondary alcohol (*iso*-propanol, *sec*-butanol, 3-pentanol, cyclohexanol), *tert*-butanol, three unsaturated alcohols (benzyl alcohol

View Article Online
DOI: 10.1039/D6CP00887A

as simplest aryl alcohol, allyl- and propargyl alcohol), and phenol. The spectra were measured over an extended period of time. Measurements of methanol, ethanol, and *iso*-propanol were performed in 2003 using a Scienta SES200 electron analyzer, whereas the data of the remaining compounds were collected between 2013 and 2015 with a Scienta R4000 analyzer. Between them, *tert*-butanol and phenol span the range of O1s energies observed in the study. All O1s spectra are presented in Fig. S1.[†] In combination with the fitting models described in Sec.2.2, the spectra were used to determine O1s ionization energies (IE), and shifts relative to the IE of methanol (ΔI).

Alcohols and phenols (ROH) undergo significant elongation of the *R-O* bond upon O1s ionization. This may be understood within the equivalent-cores model, where the core-ionized oxygen atom O^* is represented by the singly positively-charged fluorine atom, F^+. Taking ethanol as a representative example, the O1s-ionized ethanol molecule is isoelectronic to $(EtFH)^+$, which in its lowest energy state takes on the characteristics of a weakly bound $Et^+\cdots FH$ ion-dipole complex[49]. The loss of covalency upon O1s ionization is less pronounced for methanol, yet the C–O undergoes a significant extension by some 0.2 Å. This large bond elongation is responsible for a broad and featureless Franck-Condon profile, effectively leaving the adiabatic transition with negligible intensity and shifting the attention to the mean or "vertical" ionization energy.

Experimental ionization energies are listed in Tab. 3 as obtained from spectral analyses as described in the Fitting Models section. The absolute uncertainty of these measurements is determined from a combination of the uncertainty of the CO_2 reference value, 0.017 eV,[1] and the uncertainty of the shift relative to CO_2. In Ref. 1 the vertical shifts of H_2O, CO, and O_2 relative to CO_2 were determined with an uncertainty of only 0.004 eV. For the present measurements the uncertainty in individual chemical shifts is larger than this, but still $\leq$ 0.010 eV. Consistent with this, the uncertainty in the absolute ionization energies is estimated to 0.02 eV.

For five of the alcohols, namely *iso*-butanol, n- and 3-pentanol, n-hexanol, and propargyl alcohol, their oxygen 1s photoelectron spectra have, to the best of our knowledge, not been reported before. For the other twelve compounds, it is instructive to compare our ionization energies (IE) to those from four earlier studies having 4–8 compounds in common with the present one. The comparison is facilitated by bringing the data to a common standard of calibration by drawing on a recently revised and consistent set of reference energies[1] as explained in the footnotes to Tab.3. In Fig. 6, literature O1s energies are plotted against our ionization energies for eleven alcohols and phenol. Regression lines are determined for each of the four earlier compilations and included in the figure. Except for the data from Nordfors *et al.*[42], for which the slope is 0.944, the slopes are within 2 per cent of unity. The scatter about the best-fit line is pronounced in the dataset by Benoit and Harrison (1977, n=7)[44], consistent with the larger error bar (0.10 eV) associated with those measurements. The four energies from Siggel *et al.*[41] agree closely with our values, and well within their stated error bars (0.03–0.05 eV). The ionization energies reported by Nordfors *et al.* (1991, n=8)[42] and Mills *et al.* (1976, n=5)[43] lie on average about 0.07 eV above ours, suggesting a systematic difference in experimental procedures or data analyses.

Experimentally determined chemical shifts (relative to methanol) in O1s IE are included in Tab. 4. As argued above, the uncertainty in individual chemical shifts obtained in the present study, is considered to be $\leq$ 0.010 eV. In terms of linear regression between the present and literature shift values, R^2 and slopes are as given in the insert to Fig. 6. The constant terms are 0.013 eV, i.e., just outside our error bar, based on the data in Ref. 42, and $<$ 0.005 eV if computed from the data in Refs. 41 and 43.

View Article Online
DOI: 10.1039/D6CP00887A

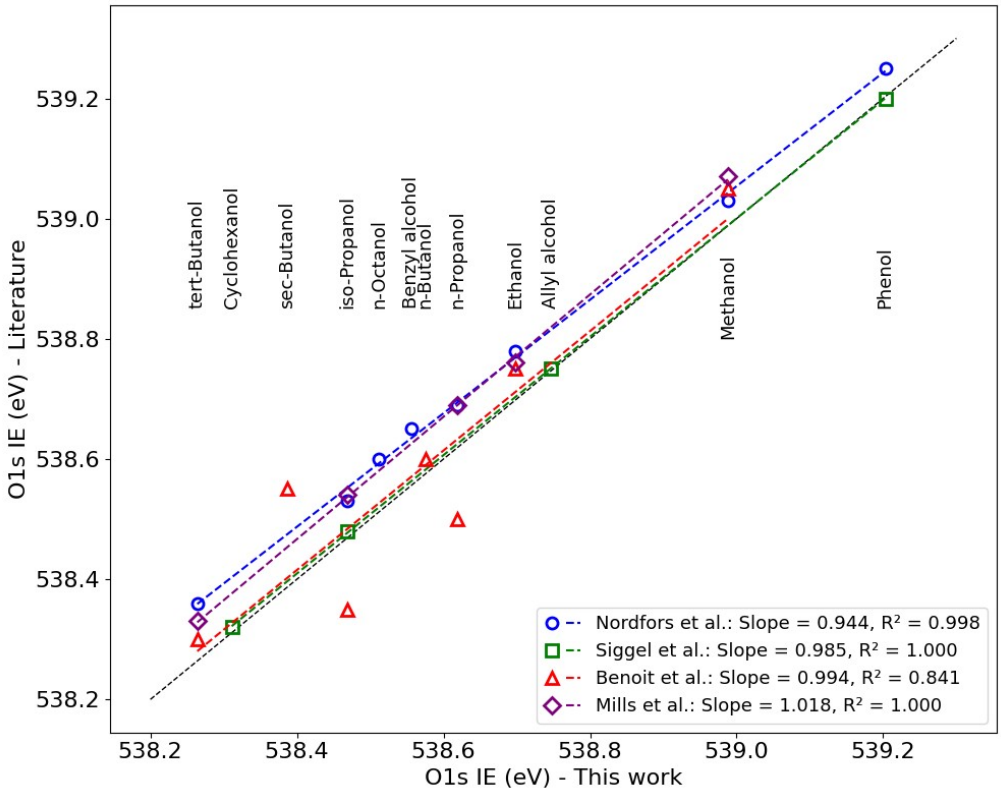

Fig. 6 Comparison of O1s ionization energies between this work (abscissa) and literature data (ordinate) by Nordfors *et al.*[42], Siggel *et al.*[41], Benoit *et al.*[44], and Mills *et al.*[43]. A least-squares line is fit to each data set, with slopes and R² values included in the legend. A 1:1 line extends beyond the data points to aid the eye.

Table 3 *Comparison of experimental oxygen 1s ionization energies (eV)*

Alcohol	This work [a]	Nordfors [b]	Siggel [c]	Benoit [d]	Mills [e]
Methanol	538.988	539.03		539.05(10)	539.07(3)
Ethanol	538.698	538.78		538.75(10)	538.76(3)
n-Propanol	538.619	538.69		538.50(10)	538.69(3)
n-Butanol	538.575			538.60(10)	
n-Pentanol	538.539				
n-Hexanol	538.529				
n-Octanol	538.512	538.60			
iso-Butanol	538.560				
iso-Propanol	538.469	538.53	538.48(3)	538.35(10)	538.54(3)
sec-Butanol	538.387			538.55(10)	
3-Pentanol	538.319				
Cyclohexanol	538.311		538.32(5)		
tert-Butanol	538.264	538.36		538.30(10)	538.33(3)
Benzyl alcohol	538.556	538.65			
Allyl alcohol	538.746		538.75(3)		
Propargyl	539.008				
Phenol	539.203	539.25	539.20(5)		

[a] Uncertainty estimated to 0.02 eV. Three decimals are retained in light of the estimated error bar of 0.010 eV in chemical shifts.
[b] Ref. 42; recalibrated from CO_2 O1s = 541.28(12) eV[51] to 541.253(17) eV[1]. No uncertainty stated.
[c] Ref 41; recalibrated from CO_2 O1s = 541.28(2) eV[52] to 541.253(17) eV[1].
[d] Ref. 44; recalibrated from CO_2 O1s = 541.3 eV[53] to 541.253(17) eV[1]. The uncertainty is estimated to ±0.1 eV by the authors.
[e] Ref. 43, recalibrated with O_2 $^4\Sigma$ O1s = 543.294(17) eV[1].

View Article Online
DOI: 10.1039/D6CP00887A

Table 4 *Comparison of experimental O1s shifts (ΔI relative to methanol, in eV)*

Alcohol	**This work**[a]	Nordfors [b]	Siggel [c]	Mills [d]
Methanol	0.000	0.00	0.00[e]	0.00
Ethanol	-0.290	-0.25		-0.31
n-Propanol	-0.368	-0.34		-0.38
n-Butanol	-0.412			
n-Pentanol	-0.449			
n-Hexanol	-0.459			
n-Octanol	-0.475	-0.43		
iso-Butanol	-0.427			
iso-Propanol	-0.519	-0.50	-0.51	-0.53
sec-Butanol	-0.601			
3-Pentanol	-0.669			
Cyclohexanol	-0.677		-0.67	
tert-Butanol	-0.724	-0.67		-0.74
Benzyl alc.	-0.432	-0.38		
Allyl alc.	-0.242		-0.24	
Propargyl alc.	0.020			
Phenol	0.215	0.22	0.21	

[a] Uncertainty $\leq$0.010 eV. [b] Ref. 42 [c] Ref. 41 [d] Ref. 43
[e] Shifts are computed using 538.988 eV for methanol (this work).

Data availability

View Article Online
DOI: 10.1039/D6CP00887A

The following data for this article are available as Electronic Supplementary Information: Extended experimental details of the recording of carbon 1s and oxygen 1s photoelectron spec tra of gaseous alcohols and phenol, graphical representation of the same spectra, and details on the computational approach to computing initial-state shifts in core 1s ionization energies. The pyEKT computer program is available from the corresponding au thor upon request. See DOI: [URL– format https://doi.org/DOI]